Universal optical transmission features in periodic and quasiperiodic hole arrays

Domenico Pacifici[1], Henri J. Lezec[1,2], Luke A. Sweatlock[1], Robert J. Walters[1], and Harry A. Atwater[1]

[1] *California Institute of Technology, 1200 E. California Boulevard, Pasadena, CA 91125, USA*
[2]*Current address: Center for Nanoscale Science and Technology, National Institute of Standard and Technology 100 Bureau Drive, Gaithersburg, MD 20899, USA*
**Corresponding author: pacifici@caltech.edu*

Abstract: We investigate the influence of array order in the optical transmission properties of subwavelength hole arrays, by comparing the experimental spectral transmittance of periodic and quasiperiodic hole arrays as a function of frequency. We find that periodicity and long-range order are not necessary requirements for obtaining enhanced and suppressed optical transmission, provided short-range order is maintained. Transmission maxima and minima are shown to result, respectively, from constructive and destructive interference at each hole, between the light incident upon and exiting from a given hole, and surface plasmon polaritons (SPPs) arriving from individual neighboring holes. These SPPs are launched along both illuminated and exit surfaces, by diffraction of the incident and emerging light at the neighboring individual subwavelength holes. By characterizing the optical transmission of a pair of subwavelength holes as a function of hole-hole distance, we demonstrate that a subwavelength hole can launch SPPs with an efficiency up to 35%, and with an experimentally determined launch phase $\varphi = \pi/2$, for both input-side and exit-side SPPs. This characteristic phase has a crucial influence on the shape of the transmission spectra, determining transmission minima in periodic arrays at those frequencies where grating coupling arguments would instead predict maxima.

©2008 Optical Society of America

OCIS codes: (240.6680) Surface plasmons; (050.1220) Apertures; (050.1950) Diffraction gratings; (260.1960) Diffraction theory; (260.3160) Interference; (999.9999) Aperiodic gratings.

References and links

1. H. A. Bethe, "Theory of diffraction by small holes," Phys. Rev. **66**, 163-182 (1944).
2. C. J. Bouwkamp, "On Bethe's theory of diffraction by small holes," Philips Res. Rep. **5**, 321-332 (1950).
3. T. W. Ebbesen, H. J. Lezec, H. F. Ghaemi, T. Thio, and H. J. Wolff, "Extraordinary optical transmission through sub-wavelength hole arrays," Nature **391**, 667-669 (1998).
4. H. F. Ghaemi, T. Thio, D. E. Grupp, T. W. Ebbesen, and H. J. Lezec, "Surface plasmons enhance optical transmission through subwavelength holes," Phys. Rev. B **58**, 6779-6782 (1998).
5. H. Raether, *Surface Plasmons on Smooth and Rough Surfaces and on Gratings* (Springer-Verlag, Tracts in Mod. Phys., Vol. 111, New York, 1988).
6. M.M.J. Treacy, "Dynamical diffraction in metallic optical gratings," Appl. Phys. Lett. **75**, 606-608 (1999).
7. M.M.J. Treacy, "Dynamical diffraction explanation of the anomalous transmission of light through metallic gratings," Phys. Rev. B **66**, 195105 (2002).
8. H. J. Lezec, and T. Thio, "Diffracted evanescent wave model for enhanced and suppressed optical transmission through subwavelength hole arrays," Opt. Express **12**, 3629-3651 (2004).
9. S.-H. Chang, S. K. Gray, and G. C. Schatz, "Surface plasmon generation and light transmission by isolated nanoholes and arrays of nanoholes in thin metal films," Opt. Express **13**, 3150-3165 (2005).
10. Y. Xie, A. R. Zakharian, J. V. Moloney, and M. Mansuripur, "Transmission of light through a periodic array of slits in a thick metallic film," Opt. Express **13**, 4485-4491 (2005).

#94182 - $15.00 USD Received 25 Mar 2008; revised 28 May 2008; accepted 28 May 2008; published 6 Jun 2008

11. M. Sun, J. Tian, Z.-Y. Li, B.-Y. Cheng, D.-Z. Zhang, A.-Z. Jin, H.-F. Yang, "The role of periodicity in enhanced transmission through subwavelength hole arrays," Chin. Phys. Lett. **23**, 486-488 (2006).
12. T. Matsui, A. Agrawal, A. Nahata, and Z. V. Vardeny, "Transmission resonances through aperiodic arrays of subwavelength apertures," Nature **446**, 517-521 (2007).
13. F. Przybilla, C. Genet, and T. W. Ebbesen, "Enhanced transmission through Penrose subwavelength hole arrays," Appl. Phys. Lett. **89**, 121115 (2006).
14. G. Gay, O. Alloschery, B. Viaris de Lesegno, C. O'Dwyer, J. Weiner, and H. J. Lezec, "The optical response of nanostructured surfaces and the composite diffracted evanescent wave model," Nature Phys. **2**, 262-267 (2006).
15. G. Gay, O. Alloschery, B. Viaris de Lesegno, J. Weiner, and H. J. Lezec, "Surface wave generation and propagation on metallic subwavelength structures measured by far-field interferometry," Phys. Rev. Lett. **96**, 213901 (2006).
16. D. Pacifici, H. J. Lezec, H. A. Atwater, "All-optical modulation by plasmonic excitation of CdSe quantum dots," Nature Phot. **1**, 402-406 (2007).
17. F. Kalkum, G. Gay, O. Alloschery, J. Weiner, H. J. Lezec, Y. Xie, M. Mansuripur, "Surface-wave interferometry on single subwavelength slit-groove structures fabricated on gold films," Opt. Express **15**, 2613-2621 (2007).
18. D. Pacifici, H. J. Lezec, H. A. Atwater, J. Weiner, "Quantitative determination of optical transmission through subwavelength slit arrays in Ag films: role of surface wave interference and local coupling between adjacent slits," Phys. Rev. B **77**, 115411 (2008).
19. A.-L. Baudrion, F. de Leon-Perez, O. Mahboub, A. Hohenau, et al., "Coupling efficiency of light to surface plasmon polariton for single subwavelength holes in a gold film", Opt. Express **16**, 3420-3429 (2008).
20. N. G. de Bruijn, "Algebraic theory of Penrose's non-periodic tilings of the plane. I-II," Mathematics Proceedings A **84**, 39-66 (1981).
21. O. T. A. Janssen, H. P. Urbach, G. W. 't Hooft, "On the phase of plasmons excited by slits in a metal film," Opt. Express **14**, 11823-11832 (2006).
22. H. J. Lezec, A. Degiron, E. Devaux, R. A. Linke, L. Martin-Moreno, F. J. Garcia-Vidal, T. W. Ebbesen, "Beaming light from a subwavelength aperture," Science **297**, 820-822 (2002).
23. P. Lalanne, J. P. Hugonin, J. C. Rodier, "Approximate model for surface-plasmon generation at slit apertures," J. Opt. Soc. Am. A **23**, 1608-1615 (2006).
24. G. Leveque, O. J. F. Martin, J. Weiner, "Transient behavior of surface plasmon polaritons scattered at a subwavelength groove," Phys. Rev. B **76**, 155418 (2007).
25. F. J. García de Abajo, "Colloquium: Light scattering by particle and hole arrays," Rev. Mod. Phys. **79**, 1267-1290 (2007).
26. C. Genet, M. P. van Exter, and J. P. Woerdman, "Huygens description of resonance phenomena in subwavelength hole arrays," J. Opt. Soc. Am. A **22**, 998-1002 (2005).
27. H. Gao, J. Henzie, and T. W. Odom, "Direct evidence for surface plasmon-mediated enhanced light transmission through metallic nanohole arrays," Nano Letters **6**, 2104-2108 (2006).

1. Introduction

The scattering of light by a subwavelength aperture, such as a hole in a metal screen, is a fundamental diffraction phenomenon that has long been the subject of scientific study [1-2]. Interesting phenomena arise when identical subwavelength apertures are periodically milled in a metal film. Indeed, periodic arrays of subwavelength holes in an opaque metal film have been shown to display strongly-modulated optical transmittance as a function of frequency [3-4]. This spectral modulation is especially pronounced for certain metals such as Ag or Au, and manifests itself as a succession of peaks and valleys related to the periodicity.

This problem has received great interest by the scientific community, and many experimental and theoretical reports have been devoted to understanding the underlying physics.

Spectral transmission maxima were first assigned to "resonant excitation" of surface plasmon polaritons (SPPs) [5]. The invocation of a resonant phenomenon was in large part motivated by the exceptionally large perceived magnitude of the peak transmission efficiencies, "about 1000 times higher than expected for subwavelength holes" [4]. Spectral transmission minima were ascribed to an unrelated phenomenon, the occurrence of tangentiality of far-field diffraction lobes ("Wood's anomaly" condition).

#94182 - $15.00 USD Received 25 Mar 2008; revised 28 May 2008; accepted 28 May 2008; published 6 Jun 2008
(C) 2008 OSA

Subsequently, other explanations were proposed, based on "dynamical diffraction" in periodic slit and hole arrays [6-7]. Recently, the magnitude of the enhanced transmission was revised substantially downwards, with both experimental [8] and numerical results [9,10] revealing maximum transmission enhancement not exceeding a factor of ~10, when properly normalized to the transmission efficiency of an isolated aperture. In addition, spectral transmission minima were shown to correspond to a condition of actual transmission suppression.

The observation of a periodic succession, as a function of wavelength, of transmission enhancements and suppressions of comparable magnitude motivated alternative interpretations based on interference and diffraction other than resonant excitation of SPPs [8].

Recent studies have shown that quasiperiodic arrays of subwavelength apertures show enhanced transmission even though they lack translational symmetry [11-13]. The transmittance of these quasiperiodic arrays has been described in terms of "resonant coupling" of the incident light with the surface plasmon modes of the metal through momentum coupling provided by the long-range periodicity of the structure [11,12]. This approach asserts that since surface plasmons are characterized by a greater wavevector than the free space photon at a given energy, a grating or other periodic structure is needed to provide the extra momentum required to resonantly couple an incident light beam to surface plasmon modes. According to this picture, a peak in the transmission spectrum of a hole array is expected at those wavelengths that fulfill the momentum matching condition [3, 4, 11, 12].

By using a specifically tailored quasiperiodic geometry, we demonstrate that significant spectral transmission modulation through an array of holes can be achieved in the total absence of translational periodicity and long-range order. We show that this observation is consistent with a simple, unified picture of transmission enhancement and suppression, valid for both periodic and aperiodic arrays, which involves interference at individual hole sites between SPPs and light incident upon or emerging from the hole. In this picture, the SPPs are generated not by the momentum provided by the periodic component of a grating (such as would be the case for example for a shallow, sinusoidal grating) but via efficient diffractive scattering into SPP modes of the incident or emerging light at the input or exit aperture of individual holes. Based on in-plane interference experiments involving pairs of subwavelength-diameter cylindrical holes, we demonstrate the efficient generation of SPPs at each hole, consistent with recent experimental results reported for subwavelength grooves [14-16], slits [17,18] , and cylindrical holes [19] milled in metal films. We measure the SPP launch phase at the input and exit aperture of a cylindrical hole, and show that it takes on a characteristic value of $\pi/2$ with respect to the phase of the incident or emerging light. A simple algebraic interference model is presented which reproduces the salient features of the transmission spectra for a variety of periodic, quasi-periodic and aperiodic arrays. This model underscores the dominant contribution of local order to the transmission properties of hole arrays, which explains how transmission modulation through periodic hole arrays can also be obtained under illumination with broad-band white-light sources of coherence length not exceeding a few lattice constants.

2. Transmission spectra of periodic and quasiperiodic hole arrays

A variety of hole arrays in a 250nm-thick Ag film evaporated onto a optically-flat fused silica microscope slide were fabricated by focused ion beam milling (Ga+ ions, 30 keV). Periodic hole arrays were generated with square and triangular lattices. In addition, two types of quasiperiodic hole arrays, lacking translational periodicity, were implemented using a generalization of the de Bruijn "cut and projection" method [20]. The first, a standard Penrose tiling of the plane, is determined by using a pentagrid in the complex plane and has both short-range and long-range order. The second, a dodecagonal tiling, is generated by using a generalized grid with 12-fold rotational symmetry (dodecagrid).

#94182 - $15.00 USD Received 25 Mar 2008; revised 28 May 2008; accepted 28 May 2008; published 6 Jun 2008
(C) 2008 OSA

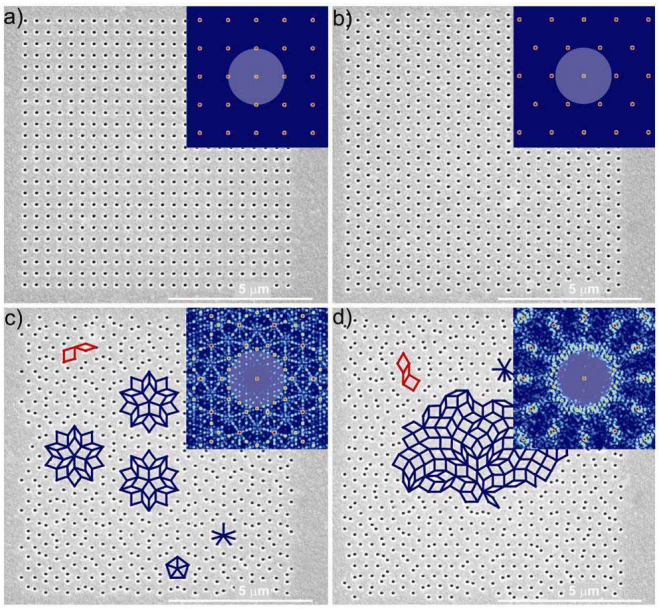

Fig. 1. SEM images of hole arrays milled in a Ag film according to (a) square, (b) triangular, (c) Penrose, and (d) dodecagonal tilings of the plane. The nearest neighbor distance (for square and triangular arrays) and side of the tiling rhombi (for quasiperiodic arrays, shown as red lines) is a=400nm. The insets show the power spectra of computed 2D discrete Fourier transforms of each array type, in a logarithmic color map scale; the superimposed gray disk has a constant radius equal to $2\pi/a$ as reference length for the reciprocal space vectors.

The dodecagonal array has been designed to lack long-range order and maintain short-range (that is, local) order only.

For all four types of arrays, the characteristic distance a between holes was systematically varied in the range 350-800 nm, in step of 50 nm, with a precision of 1%. a corresponds to the nearest-neighbor distance in periodic hole arrays (i.e., square and triangular arrays) and it is equal to the side of the "thin" and "thick" rhombi used to tile the plane in quasiperiodic hole arrays (i.e. Penrose and dodecagonal arrays). The hole diameter d was simultaneously modified to maintain a constant ratio d/a = 0.25. For normalization purposes, random arrays were generated for each hole array, by randomly displacing the hole coordinates, while keeping the hole diameter and total number of holes fixed. Each array occupies a 10×10 μm^2 area. A flat fused silica microscope slide and an optical fluid with index n = 1.46 at 514.5 nm was employed to cover the sample surface in order to index-match both sides of the Ag film.

Figure 1 shows series of scanning electron micrographs of the four different types of hole arrays generated according to square (a), triangular (b), Penrose (c), and dodecagonal (d) tilings of the plane. The four displayed arrays have the same a = 400 nm. The insets to each image show the power spectrum (in a logarithmic color scale) of the calculated 2D discrete Fourier transforms for each pattern (modeling each hole as a "point hole" unit sample function, i.e. not taking the hole diameter into account). In contrast to the case of periodic arrays, the resulting Fourier transforms of the quasiperiodic arrays are characterized by an infinitely dense discrete set of bright points, with different intensity. The lack of periodicity is clearly reflected in the Fourier transform images of (c) and (d). A striking difference yet exists between the two quasiperiodic hole arrays: while the Penrose shows bright spots within the first diffraction ring (gray disk), a clear indication of long-range order, no such spots are visible within the first diffraction ring of the dodecagonal array, indicating that the latter structure, by design, lacks both periodicity and long-range order.

#94182 - $15.00 USD Received 25 Mar 2008; revised 28 May 2008; accepted 28 May 2008; published 6 Jun 2008
(C) 2008 OSA

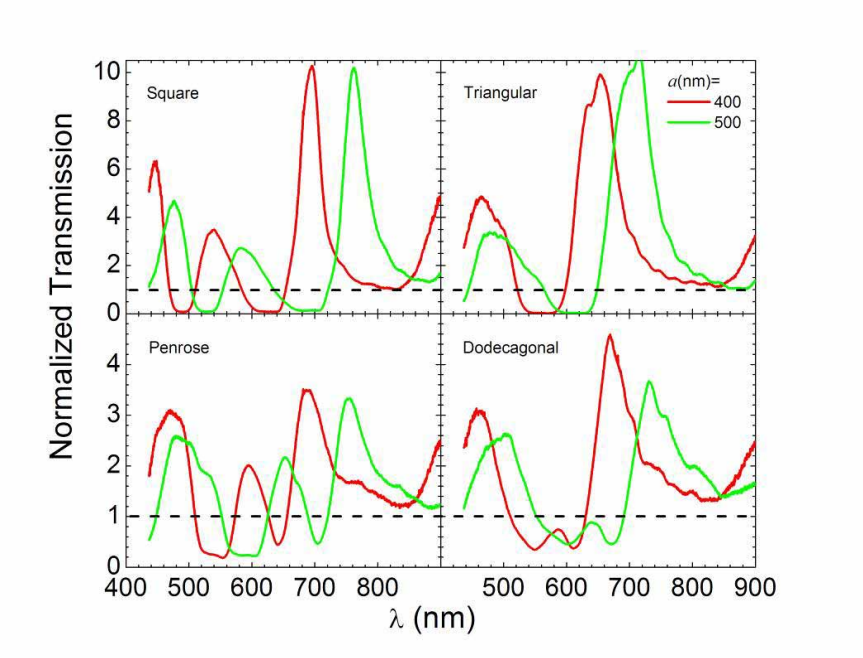

Fig. 2. Optical transmission through hole arrays with hole-hole distance a = 400 nm (red line) and a = 500 nm (green line), normalized to the measured optical transmission through random arrays with same hole diameter and number of holes.

This concept is further illustrated in real space by the blue lines superimposed on the scanning electron micrographs. While the Penrose array is composed of complex and highly symmetric patterns that repeat themselves upon rotation and translation (Fig. 1(c), blue lines), the dodecagonal array lacks such long-range order (Fig. 1(d), blue lines). Indeed its structure resembles that of a glassy matrix in which only local order and coordination number are preserved.

Transmission measurements were performed using an inverted microscope. Samples were uniformly illuminated at normal incidence using collimated light from a tungsten filament lamp. The light transmitted through each hole array was then collected by a 50X microscope objective with a numerical aperture of 0.45, dispersed using a single grating monochromator and projected onto a liquid-nitrogen-cooled CCD array detector (100×1340 pixels, 400-900 nm wavelength range). The resulting transmission spectrum of each hole array was then divided by that of the associated random array in order to obtain a "normalized" transmission spectrum as a function of λ, the free space wavelength of the incident light. This normalized transmission yields the per-hole transmission enhancement factor which results in going from a disordered to ordered array of holes. Most significantly, the normalized transmission spectrum corresponds to the per-hole transmission enhancement (or suppression) which results when an isolated hole is surrounded with an ordered array of identical holes.

In Fig. 2 we plot the normalized transmission spectrum for two fixed values of a (that is 400 and 500 nm), which displays pronounced maxima and minima, corresponding to enhancement and suppression respectively, the positions of which as a function of λ depend on the particular array, and, within the same type of array, on the hole-hole distance a. Maximum per-hole transmission enhancement factors of approximately 10, 17, 3.4 and 4.5 are observed for the square, triangular, Penrose and dodecagonal arrays, respectively. Corresponding maximum suppression factors are 0.06, 0.02, 0.15, and 0.13, respectively.

#94182 - $15.00 USD Received 25 Mar 2008; revised 28 May 2008; accepted 28 May 2008; published 6 Jun 2008
(C) 2008 OSA

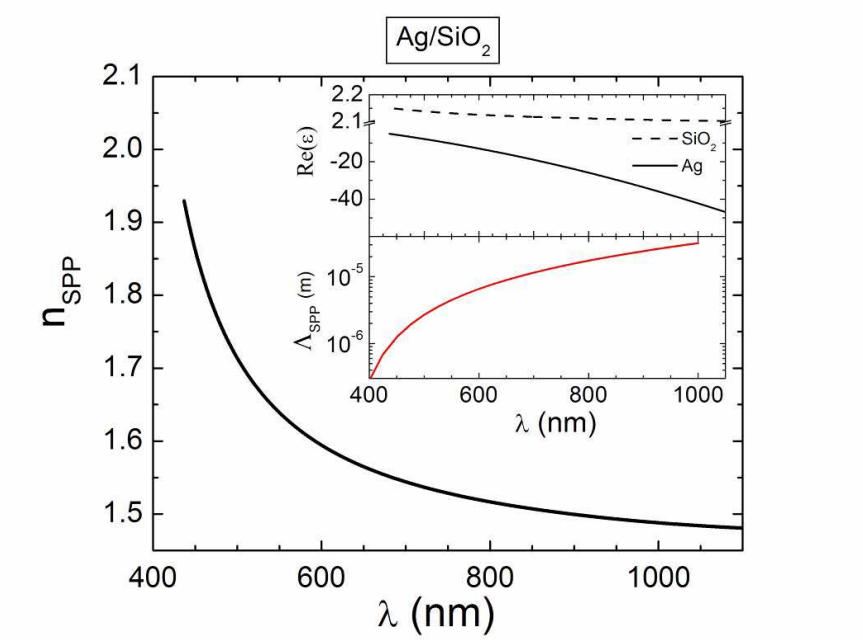

Fig. 3. Mode refractive index for surface plasmon polaritons at a Ag/SiO_2 interface, as a function of free space wavelength. Insets: top panel, real part of the dielectric constants of Ag and SiO_2 as experimentally determined by spectroscopic ellipsometry; bottom panel, SPP propagation lengths at a flat Ag/SiO_2 interface.

By increasing *a* from 400 to 500 nm, the positions of both maxima and minima shift towards longer wavelengths. It is remarkable to note that the triangular and dodecagonal hole arrays show very similar features in their normalized spectra, even though the geometries are substantially different.

Next, we search for universal trends in the normalized transmission dictated by the array geometry, independently of absolute physical dimensions (as determined by *a*) or spectral nonlinearities introduced by our specific choice of frequency range (in particular via the frequency dependence of the dielectric permittivity of the metal and dielectric). SPPs traveling along the respective metal-dielectric interfaces on both sides of the film can be expected to play a key role in the transmission modulation process, at least in the case of the periodic arrays. The SPP mode index on a given interface is frequency-dependent and given by:

$$n_{SPP}(\lambda) \equiv \frac{\lambda}{\lambda_{SPP}} = \mathrm{Re}\left[\left(\frac{\varepsilon_1(\lambda)\varepsilon_2(\lambda)}{\varepsilon_1(\lambda)+\varepsilon_2(\lambda)}\right)^{1/2}\right], \quad (1)$$

where λ_{SPP} is the effective wavelength of the in-plane-propagating SPP, ε_1 and ε_2 are the (complex) dielectric permittivity of the metal and dielectric, respectively, and Re(*z*) represents the real part of *z*. Experimental values of $\varepsilon(\lambda)$ for the evaporated Ag film and the glass substrate, respectively, are obtained using spectroscopic ellipsometry (Fig. 3, inset). Using these data we derive $n_{SPP}(\lambda)$ for the surface plasmon polariton mode bound at the Ag/SiO_2 interface (Fig. 3). The SPP mode index decreases as a function of free-space wavelength. For purposes of convenience, we assume an identical function $n_{SPP}(\lambda)$ for the SPP traveling along the boundary between Ag and the index-matched quartz slide.

#94182 - $15.00 USD Received 25 Mar 2008; revised 28 May 2008; accepted 28 May 2008; published 6 Jun 2008
(C) 2008 OSA

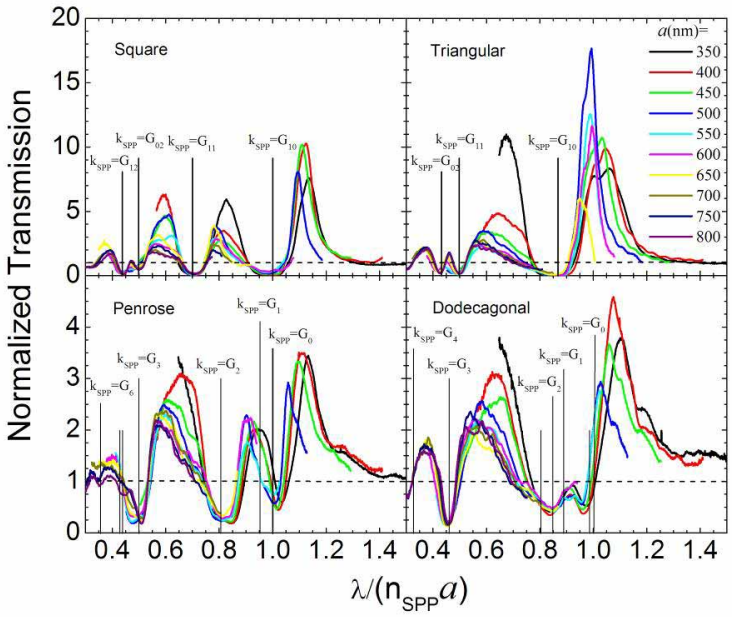

Fig. 4. Experimental universal transmission spectra for various types of hole arrays as a function of normalized wavelength.

From the measured dielectric constants we can also estimate the propagation length of a surface plasmon polariton at the Ag/SiO_2 interface, which is defined as:

$$\Lambda_{SPP}(\lambda) \equiv \frac{4\pi\kappa_{SPP}}{\lambda} = \frac{4\pi}{\lambda}\,\mathrm{Im}\left[\left(\frac{\varepsilon_1(\lambda)\varepsilon_2(\lambda)}{\varepsilon_1(\lambda)+\varepsilon_2(\lambda)}\right)^{1/2}\right], \qquad (2)$$

where $\kappa_{SPP}(\lambda)$ is the imaginary part of the complex SPP index of refraction. Values for $\Lambda_{SPP}(\lambda)$ are reported in the bottom panel inset to Fig. 3, and range from ~280 nm at λ = 400 nm to ~32 μm at λ = 1000 nm.

In Fig. 4, we plot the normalized transmission for the four different hole geometries as a function of the dimensionless quantity $\lambda/(n_{SPP}\,a) = \lambda_{SPP}/a$. In all the experiments performed in the present paper, $0.3 < \lambda_{SPP}/a < 1.4$ which means that the SPP wavelength λ_{SPP} is always commensurate to a. For each array type, the transmission spectrum retains a universal shape as a is varied, characterized in particular by fixed minima positions. We note that this shape invariability is not achieved if λ is normalized to a only. The transmission maxima do display a small shift to longer normalized wavelengths λ_{SPP}/a as a is decreased. This effect is potentially related to the fact that arrays with different distances a are made of holes with different diameters, which are in turn characterized by differing scattering efficiencies.

It is remarkable to note that for each array type, the spectral transmission data collapse onto a universal curve when plotted as a function of the surface plasmon wavelength divided by a. This normalization process in which we successfully "cancel out" a strong nonlinear functional dependence equivalent to $n_{SPP}(\lambda)$ clearly demonstrates the role of surface plasmon polaritons in shaping the transmission spectra for all four geometries.

3. Do transmission maxima result from grating coupling to SPPs?

The momentum of a surface plasmon polariton mode is greater than that of a photon of same frequency in the bulk dielectric facing the metal. Thus, light incident on a flat metal-dielectric

#94182 - $15.00 USD Received 25 Mar 2008; revised 28 May 2008; accepted 28 May 2008; published 6 Jun 2008
(C) 2008 OSA

interface cannot excite an SPP directly. One object which can mediate this coupling by providing the missing momentum is a periodic grating. For example, this method has been demonstrated in the case of a shallow, sinusoidal grating [5]. In this approach, an electromagnetic wave with wavevector **k** in the dielectric (of magnitude $k = 2\pi n_d/\lambda$, where n_d is the index of refraction of the dielectric), impinges on a metallic grating at an angle θ with respect to the sample normal. The incident light can excite a surface plasmon with wavevector $\mathbf{k}_{SPP}$ (of magnitude $k_{SPP} = 2\pi n_{SPP}/\lambda$) if the following condition is satisfied:

$$\mathbf{k}_{SPP} = \mathbf{k}_{\parallel} + \mathbf{G}\,, \tag{3}$$

where $\mathbf{k}_{\parallel}$ is the component of **k** parallel to the array surface (of magnitude $k_{\parallel} = k\sin\theta$) and **G** is a reciprocal vector of the periodic array. For example, for illumination at normal incidence ($\theta = 0$, $\mathbf{k}_{\parallel} = \mathbf{0}$) Eq. (3) becomes:

$$k_{SPP} = G\,. \tag{4}$$

In the case of a shallow sinusoidal grating along a specific direction of the surface, the grating momentum is given by $G = 2\pi/P$, where P is the period of the grating.

A prevailing explanation for the maxima in the transmission spectra of periodic arrays of subwavelength-diameter holes is that they result from wavelength-specific excitation of surface plasmon polaritons [3]. By analogy with the case of a shallow grating outlined above, these wavelengths are presumed to be restricted to those for which the incident light couples to an SPP via one of the fundamental reciprocal lattice vectors of the grating formed by the hole array (i.e. related to one of the fundamental periodicities of the grating in two dimensions). The implication of this approach is that the hole array can be adequately modeled as a periodic collection of "point-holes" (unit sample functions).

Thus, in this standard "point-hole" grating-coupling picture, the only grating vector assumed to have a role in the coupling process is the grating vector G related to the periodicity of the structure. For a square array of mathematical points with period a, G is given by:

$$G_{ij} = \frac{2\pi}{a}\sqrt{i^2 + j^2}\,, \tag{5}$$

Where i and j are integers (with $i \geq 0$, $j > 0$). Eqs. (4) and (5) then yield the normalized wavelengths $\lambda_{\max}/(n_{SPP}\,a)$ at which transmission maxima are predicted to occur:

$$\left(\frac{\lambda_{\max}}{n_{SPP}a}\right)_{ij} = \frac{1}{\sqrt{i^2 + j^2}}\,, \tag{6}$$

For a triangular lattice with period a, G is given by:

$$G_{ij} = \frac{4\pi}{a\sqrt{3}}\sqrt{i^2 + j^2 + ij}\,, \tag{7}$$

i and j are integers (with $i \geq 0$, $j > 0$). Eqs. (4) and (7) then yield the normalized wavelengths $\lambda_{\max}/(n_{SPP}\,a)$ at which transmission maxima are predicted to occur:

$$\left(\frac{\lambda_{\max}}{n_{SPP}a}\right)_{ij} = \frac{\sqrt{3}}{2\sqrt{i^2 + j^2 + ij}}\,, \tag{8}$$

The values of $\lambda_{\max}/(n_{SPP}\,a)$ predicted by Eqs. (7) and (8) for the square and triangular hole arrays, respectively, are indicated in Fig. 4 by vertical lines. Remarkably, in each case, the momentum matching condition fails at predicting the position of the transmission maxima.

#94182 - $15.00 USD Received 25 Mar 2008; revised 28 May 2008; accepted 28 May 2008; published 6 Jun 2008
(C) 2008 OSA

Instead, the calculated values λ_{max} /(n_{SPP} a) coincide very precisely with the experimental transmission minima.

We furthermore note that, contrary to what is implicitly assumed in Ref. [3], a grating-coupling equation such as Eq. (3) would not satisfactorily deal with an essential component contributing to the transmission spectrum of periodic arrays of subwavelength holes: surface plasmon activity on the exit side of the array. That such exit-side SPPs are present and play an equally important role in shaping the transmission spectra as the front-side SPPs evoked above is well established, for example based on experimental characterization of arrays in which the index of refraction of the dielectric medium facing the exit-side metal surface is different from that facing the input-side metal surface [3]. Two distinct and independent sets of transmission minima and maxima, of comparable magnitude, are then observed, each associated with respective sides of the film, and thus with SPPs on the respective sides. A coupling equation such as Eq. (3) cannot model the generation of exit-side SPPs since there is no incident plane wave on that side of the film. The only relevance of Eq. (3) when applied to the exit side of the film would be to model how *pre-existing* SPPs on the exit side out-couple into free space. It has nothing to say however about how those SPPs appear in the first place.

Finally, the grating coupling hypothesis is even less likely to apply in the case of the Penrose and the dodecagonal hole arrays, which have no translational periodicity.

Recently, the spectral enhancement and suppression of transmission through a Penrose array has been explained in terms of the quasiperiodic nature of the array (once again treated as a collection of mathematical points), which causes the appearance of point-like diffraction patterns in the Fourier transform [13]. According to this point of view, the electromagnetic wave impinging on the sample couples to SPPs via an effective grating vector in momentum space caused by the long range order of the Penrose tiling of point holes. However, this theory is inconsistent with the appearance of maxima and minima in the transmission spectra of our dodecagonal hole array, which has been opportunely generated to lack long-range order (as demonstrated by the presence of a broad diffraction ring and by the absence of sharp diffraction spots within the first diffraction ring). The dodecagonal array we designed is remarkably different from the dodecagonal array studied for example by Matsui et al., Ref. [12]. While both structures belong to the broad class of quasiperiodic tilings of the plane with 12-fold rotational symmetry, the dodecagonal array investigated in Ref. [12] can clearly be generated by a periodic translation of a unit cell comprising a few holes (represented in gray in Fig. 2(d) of Ref. [12]). This imposed periodicity determines a structure characterized by long-range order in real space and bright spots in its reciprocal space Fourier transform power spectrum (Fig. 2(e), Ref. [12]). In contrast, our dodecagonal array has no sign of any particular subunit cell that by simple translation could map the entire structure in real space (Fig. 1(d), blue lines). Indeed, the structure was explicitly generated to resemble a glassy matrix in which only local order and coordination number are preserved. That this structure contains a higher degree of disorder is further confirmed by the diffuse broad diffraction ring observed in its 2D discrete Fourier transform and by the absence of bright spots within this first diffraction ring (Fig. 1(d), inset).

In contrast to the periodic case, no exact analytical formula exists to index the reciprocal wavevectors of quasiperiodic hole arrays, whose reciprocal space is characterized by an infinitely dense discrete set of bright points, with orders-of-magnitude variation in intensity. However, the brightest spots in the diffraction spectra can be assigned to simple geometric distances in real space (for example the side a and semi-diagonals, respectively, of the thin and thick rhombi used to tile the plane, and represented by red lines superimposed to the SEM images in Fig. 1). For the dodecagonal array we notice that the reciprocal space is characterized by a broad diffraction ring, and a series of diffraction spots lying further out in k-space, arranged according to dodecagonal symmetry. From a direct inspection of the Fourier transform images, we can evaluate the magnitude of each such wavevector defined as G_m, with m = 0, 1, 2, … (m = 0 corresponding to the real space distance a). Then, using Eq.

#94182 - $15.00 USD Received 25 Mar 2008; revised 28 May 2008; accepted 28 May 2008; published 6 Jun 2008
(C) 2008 OSA

(4), we can calculate the normalized wavelengths $\lambda_{max}/(n_{SPP}\, a)$ at which transmission maxima might be expected to occur. The calculated normalized wavelength values are reported in Fig. 4, and correspond to transmission minima or inflexion points rather than maxima.

In summary, the canonical explanation of transmission maxima by grating coupling to SPP appears inadequate on three accounts when applied to arrays of periodic subwavelength holes:

(1) The corresponding free-space wavelengths yield transmission minima, not maxima, in periodic hole arrays, and predicts minima or inflexion points in quasiperiodic hole arrays.

(2) Such a theory does not model the excitation of output-side SPPs, the activity of which lead to transmission spectral features nevertheless identical to those resulting from SPP activity on the input surface.

(3) Similar features show up in the case of aperiodic arrays with only local order and no long range order, and hence no well-defined grating momentum.

From the results of section 2, it is clear that surface plasmon polaritons play an essential role in the transmission process of subwavelength holes arrays, both periodic and aperiodic. This raises the question of how the SPPs are actually generated. Recently it has been shown experimentally that a single subwavelength slit or groove in a Ag film could act as an efficient source of SPPs on the flat surfaces surrounding both the input and exit apertures, at various wavelengths [16-18,21]. It has also been experimentally inferred that a single cylindrical subwavelength hole in a Ag could efficiently launch an SPP on its exit side [22].

Here we propose that the SPPs on both periodic and aperiodic hole arrays are generated at all frequencies, on an individual basis at each hole. The SPPs are excited on both sides of the film when light diffracts from the input or output aperture of each hole. The necessary momentum is provided by the high spatial frequencies of the holes themselves, which are abrupt subwavelength scale interruptions in the metal surface. This view is consistent with recent theoretical reports [23,24] which show that the weighted continuum of spatial frequencies (i.e. momentum) which characterize a subwavelength slit is able to couple light very efficiently into a single SPP mode of wavevector $k_{SPP}(\lambda)$.

Once the SPPs are present it can not be taken as an *ad-hoc* assumption that this will necessarily lead to enhanced transmission. From an electromagnetic viewpoint, a hole array is a very open three-dimensional system (with short lifetimes evident from broad spectral features), as opposed to two-dimensional closed resonators (with long lifetimes and sharp spectral features). In particular, in addition to the in-plane SPPs, one must take into account the "direct" out-of-plane wave components, those impinging on the hole and emerging from the hole, respectively. We propose that it is primarily the first-order interference, between SPPs and these out-of-plane components, at the subwavelength scattering sites formed by the hole openings on respective surfaces, which gives rise to the observed transmission modulation as a function of wavelength.

4. Deconstructing the hole array: optical transmission of isolated hole pairs

In order to deconstruct (and later reconstruct) the transmission spectra of subwavelength hole arrays, we studied the transmission properties of a simpler system, that is a pair of two holes milled into a Ag film sandwiched between two fused silica microscope slides. The film thickness was 250 nm, the hole diameter was 50 nm, and the hole-hole distance *a* was varied in the range 150-1000 nm, in steps of 5 nm. A schematic cross section of the hole-hole pair is reported in Fig. 5(a). The transmission measurement setup consists of a TEM_{00} light beam from an Ar ion laser (λ = 514.5 nm, 5 mW), aligned to the optical axis of the inverted microscope.

#94182 - $15.00 USD Received 25 Mar 2008; revised 28 May 2008; accepted 28 May 2008; published 6 Jun 2008
(C) 2008 OSA

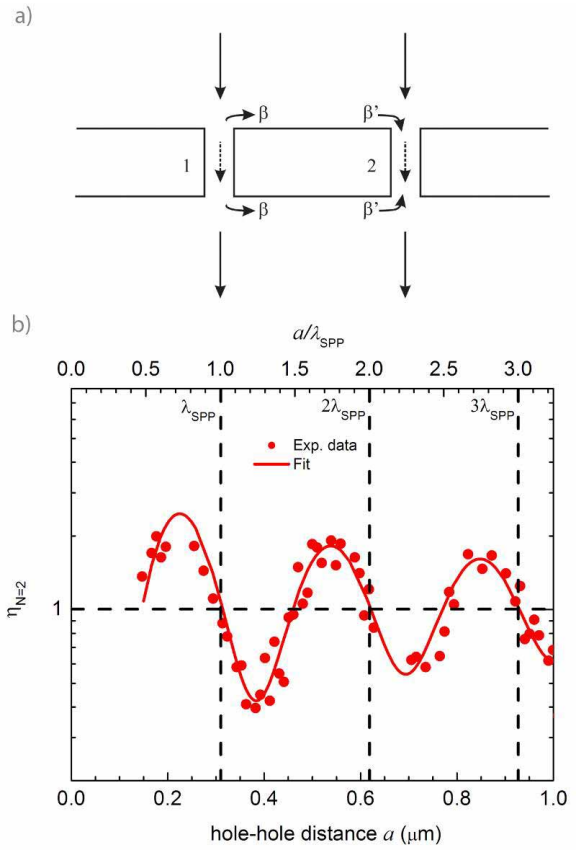

Fig. 5. Optical transmission through two holes milled in a Ag film, index matched with an optical fluid and a glass slide (both with n=1.46 at 514.5 nm) measured by uniformly illuminating the structures with a gaussian TM-polarized laser at 514.5 nm. The hole diameter is 50 nm and it is kept constant as a function of hole-hole distance a. The transmission data were opportunely normalized to extract the per-hole intensity η.

The beam is focused at normal incidence onto the sample surface through the microscope condenser, resulting in a Gaussian spot with beam waist of ~100 μm, and polarized with the electric field parallel to the mathematical line joining the centers of the two holes. The light transmitted through each hole pair is then gathered by a 50X microscope objective with a numerical aperture of 0.45 and directly detected with the same CCD as described in section 2. The transmitted light intensity is obtained by integrating the signal over the entire region of interest in the CCD image and subtracting the background originating from electronic noise.

The per-hole transmission enhancement factor is obtained by correcting the transmitted intensity for the collection efficiency of the objective lens (taking into account the three-dimensional diffraction pattern of the hole pair) and then normalizing the transmitted intensity to that collected from a single, isolated hole.

The structured Ag layer was covered by index-matching fluid (with index of refraction n = 1.46) and a second microscope slide; in this manner, the permittivity of the dielectric facing both sides of the metal film is identical. In the present experiments the complex dielectric constant of the structured silver sample was measured directly by ellipsometry at λ = 514.5 nm and determined to be $\varepsilon_{Ag} = -9.3 + 0.18i$. The dielectric constant of both fused silica

#94182 - $15.00 USD Received 25 Mar 2008; revised 28 May 2008; accepted 28 May 2008; published 6 Jun 2008
(C) 2008 OSA

substrate and index matching fluid is given by $\varepsilon_{SiO2} = +2.13$. Based on these values for ε_{Ag} and ε_{SiO2}, Eq. (1) yields an SPP wavelength $\lambda_{SPP} = 309$ nm (±1 nm as determined by statistical average over the entire surface of the film). Figure 5(b) reports the resulting per-hole transmission enhancement factor as a function of hole-hole distance. The experimental data (symbols) show an oscillatory behavior as a function of distance, with decreasing amplitude. To model the fundamental transmission behavior of the pair of holes we propose a simple surface-wave mediated interference model, in which the direct illumination of the holes plays a significant role.

Let us consider two cylindrical holes ($N = 2$), with center-to-center distance a, milled in an optically thick metal film facing identical dielectric media on either side. The top surface is uniformly illuminated by a coherent laser beam with free-space wavelength λ. The following first-order processes are proposed to occur (as illustrated in Fig. 5(a)):

(1) Each hole scatters the incident field (of effective magnetic field amplitude H_0) with an efficiency β into an SPP propagating along the top metal-dielectric interface; in other words SPPs are launched by individual holes.

(2) The SPP accrues a phase shift of $k_{SPP}\, a$ as it propagates from one hole to the other. Due to the circular expansion of the SPP, the SPP amplitude decreases by a factor of $1/(a)^{1/2}$ during its trip between the two holes.

(3) Upon reaching the second hole, the SPP field is "captured" with efficiency β' and interferes with the beam directly incident upon the hole.

(4) A fraction of this interfered field is evanescently channeled into the hole and transmitted to the bottom opening with complex transmission coefficient T.

(5) The processes (1)-(3) repeat at the bottom surface. The net interfered field at each hole aperture on the bottom surface is then scattered into free space.

Coefficients β, β' and T are complex numbers which take into account any intrinsic phase shift in the scattering and transmission processes.

The total magnetic-field immediately above the bottom aperture of either hole and resulting from this first-order interference process, is given by the following expression:

$$H_{N=2} = \left(H_0 + \frac{\beta\beta'}{\sqrt{a}} e^{ik_{SPP}a} H_0 \right) T \left(1 + \frac{\beta\beta'}{\sqrt{a}} e^{ik_{SPP}a} \right) = H_0 T \left(1 + \frac{\beta\beta'}{\sqrt{a}} e^{ik_{SPP}a} \right)^2 , \quad (9)$$

The magnetic field immediately above the output aperture of an isolated hole ($N = 1$) is given by:

$$H_{N=1} = H_0 T , \quad (10)$$

We define a per-hole transmission enhancement factor η as the ratio between the square of the field above the output aperture of a hole in a two-hole configuration ($|H_{N=2}|^2$) divided by the square of the field above the output aperture of an isolated hole ($|H_{N=1}|^2$):

$$\eta_{N=2} = \frac{|H_{N=2}|^2}{|H_{N=1}|^2} = \left| \left(1 + \frac{\beta\beta'}{\sqrt{a}} e^{ik_{SPP}a} \right)^2 \right|^2 , \quad (11)$$

The product $\beta\beta$' can be expressed as:

$$\beta\beta' = \beta_0 \beta_0' e^{i\varphi} , \quad (12)$$

where β_0 and β'_0 are real quantities and φ is a characteristic "intrinsic" phase shift resulting from the SPP emission and capture process on a given side of the film. Equation (11) can be rewritten as:

#94182 - $15.00 USD Received 25 Mar 2008; revised 28 May 2008; accepted 28 May 2008; published 6 Jun 2008
(C) 2008 OSA

$$\eta_{N=2} = \frac{|H_{N=2}|^2}{|H_{N=1}|^2} = |(1+\frac{\beta_0\beta_0^{'}}{\sqrt{a}}e^{i\varphi}e^{ik_{SPP}a})^2|^2 = \left[1+\frac{(\beta_0\beta_0^{'})^2}{a}+2\frac{\beta_0\beta_0^{'}}{\sqrt{a}}\cos(k_{SPP}a+\varphi)\right]^2, \quad (13)$$

The model of Eq. (13) is then compared to the experimental data of Fig. 5(b), using $\beta_0\beta'_0$ and φ as fitting parameters. An excellent match, plotted as the solid line in Fig. 5(b) is obtained by choosing:

$$\beta_0\beta_0^{'} = 0.12, \quad \varphi = \frac{\pi}{2}, \quad (14)$$

These values for $\beta_0\beta'_0$ and φ are obtained with precisions of ±0.01 and ±0.04, respectively. From Eq. (14) we deduce that a single hole can generate SPPs at 514.5 nm with an efficiency of β_0 = 35% in field amplitude.

Significantly, at hole-hole distances a equal to λ_{SPP} and $2\lambda_{SPP}$, respectively, we obtain $\eta_{N=2} = 1$, corresponding to a condition of neither transmission enhancement nor suppression (instead of, for example, a maximum, as might be expected for a simple two dipole system placed one effective wavelength apart, see for example Fig. 16(b), Ref. [25]). The first maximum in transmission as a function of hole-hole distance occurs at the smaller value a = (3/4) λ_{SPP}. In other words, for a given hole-hole distance a, a transmission maximum would occur at a "redshifted" free space wavelength yielding λ_{SPP} = (4/3) a.

The interference model of Eq. (13), underscores the contribution of two essential factors in shaping the transmission spectrum of the most basic array consisting of two holes:

(1) A significant field amplitude contribution from the incident and emerging light (term "1" in Eq. (13)); without this out-of-plane contribution to the interference process, the normalized transmission function $\eta_{N=2}$ (a) (corresponding to first-order interference processes) would be flat.

(2) A characteristic, "intrinsic" non-zero net phase shift φ experienced by the SPP upon launching from and collection by each hole; this phase shift is revealed by the reference phase provided by the out-of-plane components (incident beam) which also participate in the process.

The specific value of φ resulting in the case of round holes, π/2, leads to significant displacement of the transmission maxima away from the condition $\lambda_{SPP} = a$. Stated differently, the intrinsic phase shift φ increases the "effective" optical path between the two holes from a to (4/3) a.

5. Reconstructing the hole array transmission: interference model

We generalized the interference model to the case of a finite number of holes arranged according to different 2D lattices. Following the lines of thought reported previously, we assume that an incident plane wave is coupled into a surface wave upon diffractive scattering by each hole (each hole is considered as a single point scatterer). Differently from Ref. [8], here we assume that each hole is the source of propagating surface plasmon polaritons, rather than composite diffracted evanescent waves. Moreover, we explicitly consider the π/2-phase shift of the surface plasmon upon launching, which was previously neglected in [26], and which has been experimentally determined in the present paper. Each hole is therefore modeled as a source of circular waves, which propagate with a wavelength equal to that of a surface plasmon polariton (λ_{SPP}), and with a phase shift of π/2. The surface plasmon polaritons propagate along the metal surface, and interfere with the incident field at the input side of any hole in the array. We calculate the total field at each hole position, as the sum of the incident field and the surface plasmon contributions launched by all of the other holes in

#94182 - $15.00 USD Received 25 Mar 2008; revised 28 May 2008; accepted 28 May 2008; published 6 Jun 2008
(C) 2008 OSA

the array. We take into account the polarization of the incident beam. We repeat the same process at the output surface, thus determining the total field at the output mouth of each hole.

Let us define a Cartesian system of reference *xOy* in such a way that the *x* axis lays along the horizontal direction of the hole arrays represented in Fig. 1. To fix the ideas we can choose the first bottom-left hole of each array as the origin of the coordinate system. The *z* axis is normal to the array plane. An electromagnetic wave impinges upon the hole arrays at normal incidence, and polarized such that the electric field *E* oscillates in a plane forming an angle θ_p with respect to the *z*-*x* plane. Each hole can be modeled as a point dipole source located at $P_m = (x_m, y_m)$, emitting surface plasmon polaritons along the plane with a Lambert's cosine law, as experimentally demonstrated in Ref. [27]. Assuming, for simplicity of writing, $H_0 = 1$ and $T = 1$, the total field at the input side mouth of a hole located at P_m (top surface) is therefore given by:

$$H_{m,top} = 1 + \sum_{j \neq m} \frac{\beta_0 \beta_0^{'} \cos^2(\theta_{jm} - \theta_p)}{\sqrt{a_{jm}}} \exp\left[i(k_{SPP} a_{jm} + \varphi) \right], \tag{15}$$

where now "1" represents the amplitude of the incident field H_0, and the sum takes into account all of the SPP contributions originating by all of the holes located at P_j, with $j \neq m$. Here $k_{SPP} = (2\pi/\lambda)(n_{SPP} + i\ \kappa_{SPP})$ represents the complex SPP wavevector, $a_{jm} = P_j P_m$ is the distance between points P_j and P_m, and θ_{jm} is the angle formed by the vector $(\boldsymbol{P}_m - \boldsymbol{P}_j)$ and the *x* axis, with $x_m - x_j = a_{jm} \cos\theta_{jm}$. The total field at the output mouth of the *m*-th hole (bottom surface) is therefore given by:

$$H_{m,bot} = H_{m,top} + \sum_{j \neq m} \frac{\beta_0 \beta_0^{'} \cos^2(\theta_{jm} - \theta_p)}{\sqrt{a_{jm}}} H_{j,top} \exp\left[i(k_{SPP} a_{jm} + \varphi) \right] \tag{16}$$

where $H_{j,top}$ is calculated using Eq. (15). Generally, $\beta_0\beta'_0$ depends on incident wavelength and hole diameter. In the following, as an approximation, we assume a constant value for $\beta_0\beta'_0$, given by Eq. (12) and by the best-fit values reported in Eq. (14). This assumption does not affect the position of maxima and minima, its main influence being mostly in a slight variation of the absolute intensity enhancement and suppression at various wavelengths.

Experimentally we have access to the zeroth-order transmission, or per-hole transmission, η_N through an array of *N* holes, which is equal to the absolute value of the sum of the fields at the output of each aperture, squared, and normalized by the square of the total number *N* of holes in the array:

$$\eta_N = \frac{\left| \sum_{m=1}^{N} H_{m,bot} \right|^2}{N^2}. \tag{17}$$

Equation (17) generally depends on the polarization angle θ_p. In order to compare the calculated spectra with the experimental transmission spectra, which were taken using unpolarized white light illumination, we averaged Eq. (17) over the polarization angle from 0 to 2π.

The results of such an exercise are shown in Fig. 6 for a number of holes $N = 49$ and for each array type (red lines) and compared to the experimental universal transmission curves for arrays with $a = 500$ nm (blue lines). Interestingly, the calculated curves very well reproduce the main spectral features of the experimental transmission data, such as number of peaks, and positions of minima and maxima.

#94182 - $15.00 USD Received 25 Mar 2008; revised 28 May 2008; accepted 28 May 2008; published 6 Jun 2008
(C) 2008 OSA

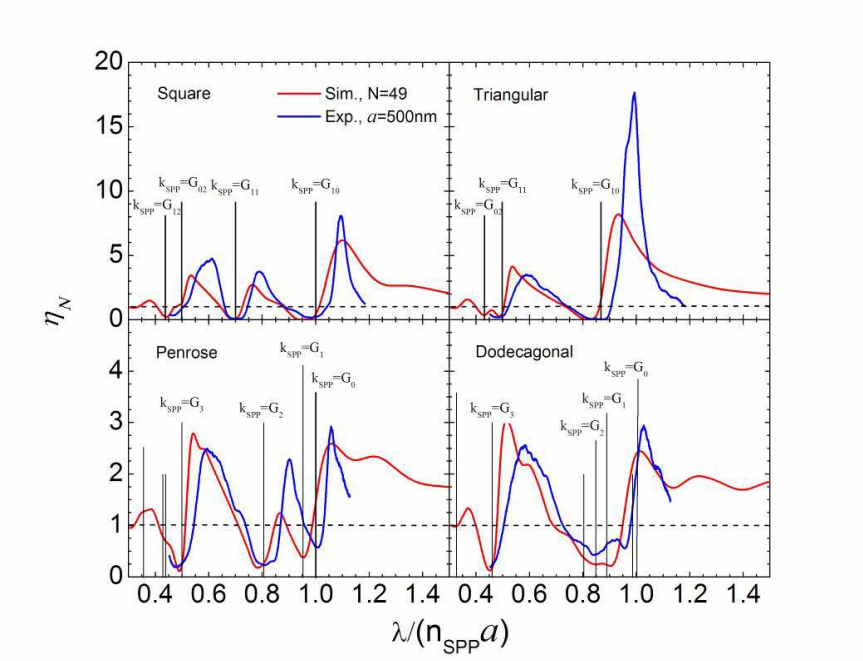

Fig. 6. Blue lines: universal transmission spectra calculated within the interference model developed in the present manuscript, using a number of holes $N = 49$. For comparison, the red solid lines represent experimental transmission data taken from Fig. 4.

The agreement is even more striking given that no free parameters have been used in the calculation, the only input parameters being the positions of the holes in each array, and the experimentally determined dielectric constants, launch phase shift and scattering efficiencies. It is worth noting that even though the fabricated arrays contained as many as 400 holes, only as few as 7 holes per side are needed to determine the transmission features experimentally observed, thus confirming that the enhanced and suppressed transmission process is indeed a strongly localized one. Only near-neighbor contributions seem to play a role in shaping the overall interference spectra.

To further investigate the role of short-range as opposed to long-range order, we measured the optical transmission of hole arrays by using light sources with different coherence lengths.

Just like in many earlier studies [3,8], in Figs. 4 and 6 we used a tungsten lamp to illuminate the hole arrays. The spatial coherence length of the lamp, taking into account the spectral resolution of the grating in our monochromator (150 lines/mm), is ~2 μm, as determined by performing transmission measurements through 1D surface wave interferometers as a function of interferometer length. On the other hand, lasers can reach spatial coherence lengths of several meters, i.e. orders of magnitude longer than the typical array dimensions and pitch. Therefore the use of a laser source would enable coherent illumination of the entire hole array pattern, and thus give rise to coherent contributions from all of the holes in the array. On the other hand, the coherence length of our lamp source is much smaller than the array size but is larger than the hole-hole distance *a*. Thus transmission spectra for lamp illumination are inherently sensitive to short-range order but not long-range order in each hole array. Figure 7 reports a comparison of the transmission intensities measured at 514.5 nm on various hole arrays using both a lamp source and an Ar laser. It is interesting to note that the general trend of array transmission measured at 514.5 nm versus distance *a* is similar for both laser and lamp illumination sources, as reported in Fig. 7. Interestingly, the square and the Penrose array show a reduced transmission when coherently illuminated.

#94182 - $15.00 USD Received 25 Mar 2008; revised 28 May 2008; accepted 28 May 2008; published 6 Jun 2008
(C) 2008 OSA

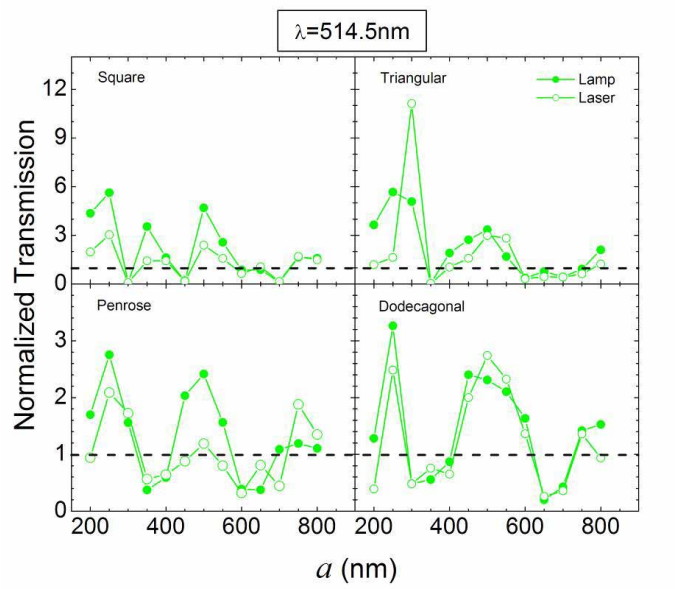

Fig. 7. Normalized optical transmission measured at λ=514.5nm for various types of hole arrays. A coherent Ar laser source and an incandescent lamp have been used. The coherence length of the lamp and spectrometer system was experimentally determined to be ~2μm.

The dodecagonal array does not show any substantial difference in spectral transmission for coherent versus partially-coherent illumination. This result supports the conclusion that experimental hole array spectral transmission is dominated by short-range order rather than long-range order.

This result is not at all surprising. Indeed, the SPP contributions arriving at a given hole and originating from distant holes are strongly attenuated by the $1/(a)^{1/2}$ functional dependence of the launched SPP field amplitude, as determined by the two-hole experiment reported in Fig. 5(b) of this paper. Therefore, distant holes do not effectively contribute to the per-hole enhancement or suppression. Moreover, SPPs generated at the metal/dielectric surface are attenuated by material loss in the metal, which determine propagation lengths Λ_{SPP} of the order of a few hundreds of nanometers up to tens of micrometers, depending on the frequency. As reported in the inset to Fig. 3, the propagation length for an SPP propagating at a flat Ag/SiO_2 interface in our samples is >10 μm (i.e. longer than the array lateral size) only for $\lambda > 670$ nm. At $\lambda = 514.5$ nm the propagation length is $\Lambda_{SPP} = 3.2$ μm. For an array with hole-hole distance $a = 500$ nm this means that roughly 6-7 holes per side would effectively contribute to the per-hole enhancement (or suppression) factor, without taking into account the stronger $1/(a)^{1/2}$ dependence. As an additional contribution to the localized nature of the per-hole transmission, we have to consider that SPPs originating from distant holes can suffer out-of-plane scattering by finite-size holes encountered along their in-plane propagation path. While a point-like hole would be characterized by a very small (virtually zero) in-plane scattering cross section, a hole with a finite diameter acts as an efficient scattering center for the in-plane propagating surface plasmon, with consequent additional "screening" of SPP contributions originating from distant holes.

4. Conclusions

We have found that the overall experimental transmission features, including the positions of maxima and minima, of subwavelength hole arrays depend only on the hole-hole distance *a*, the surface plasmon mode refractive index, the in-plane hole distribution and position, and a characteristic phase shift for the launched surface plasmon. By plotting the normalized

#94182 - $15.00 USD Received 25 Mar 2008; revised 28 May 2008; accepted 28 May 2008; published 6 Jun 2008
(C) 2008 OSA

transmission for different hole geometries as a function of a dimensionless quantity λ_{SPP}/a we found universal spectral curves, independent of array pitch *a*, thus confirming the crucial role played by surface plasmon polaritons in the observed enhanced and suppressed optical transmission. We experimentally determined a phase shift of $\pi/2$ upon scattering of the incident beam into a surface plasmon polariton. The appearance of minima, instead of maxima, at those wavelengths corresponding to the grating coupling condition results from destructive interference of SPP contributions originating from the 2D distribution of neighboring holes. We found that this characteristic phase shift does not depend on film thickness (hole depth), nor on the hole size (provided the hole diameter can still be considered "subwavelength") while it depends on the shape of the aperture. Indeed, by performing optical transmission measurements through slit arrays as a function of slit number and slit-slit separation distance, we determined a π-phase shift for an SPP launched by a long slit with subwavelength width [18]. These experiments prove that different launching geometries are intrinsically characterized by different phase slips upon launching. In fact long, narrow slits act like line dipole sources which launch surface plane waves, while subwavelength circular holes act as point dipole sources which launch surface cylindrical waves. The apparent phase slip therefore results from the projection of outgoing cylindrical waves into the surface plane wave basis. We investigated the role of long-range and short-range order effects by comparing the transmission properties of periodic and quasiperiodic subwavelength hole arrays, illuminated with both coherent and partially-coherent light. The presence of transmission maxima in quasiperiodic hole arrays strongly suggests that short-range rather than long-range order is responsible for the enhanced and suppressed transmission. These results are consistent with: (1) the $1/(a)^{1/2}$ functional dependence of the launched SPP field amplitude, (2) the relatively short propagation distances of SPPs at a Ag/SiO_2 flat interface, and (3) the expectation that subwavelength holes with a finite diameter in a metal film are strong out-of-plane scatterers for propagating surface plasmons. We explain the spectral transmittance of hole arrays in metal films as the result of interference between directly transmitted light incident on subwavelength holes and individual surface plasmons generated by diffractive scattering from neighboring holes. We show that the proposed model for spectral transmission can be successfully applied to reproduce the transmission properties of arrays of subwavelength holes irrespective of their lattice type and degree of order, without recurring to *ad-hoc* assumptions or fitting parameters.

Acknowledgements

We acknowledge from the Department of Energy, Basic Energy Sciences program under grant DOE DE-FG02-07ER46405.

#94182 - $15.00 USD Received 25 Mar 2008; revised 28 May 2008; accepted 28 May 2008; published 6 Jun 2008
(C) 2008 OSA